IBM-1 calculations towards the neutron-rich nucleus ^{106}Zr

Stefan Lalkovski[1,2,3] and P. Van Isacker[3]
[1] *Faculty of Physics, University of Sofia, Sofia, BG-1164 Bulgaria*
[2] *School of Environment and Technology, University of Brighton, Brighton BN2 4JG, UK*
[3] *Grand Accélérateur National d'Ions Lourds, CEA/DSM–CNRS/IN2P3, BP 55027, F-14076 Caen Cedex 5, France*
(Dated: March 23, 2009)

The neutron-rich $N = 66$ isotonic and $A = 106$ isobaric chains, covering regions with varying types of collectivity, are interpreted in the framework of the interacting boson model. Level energies and electric quadrupole transition probabilities are compared with available experimental information. The calculations for the known nuclei in the two chains are extrapolated towards the neutron-rich nucleus ^{106}Zr.

PACS numbers:

I. INTRODUCTION

In the last decade the neutron-rich nuclei in the $40 \leq Z \leq 50$ region have attracted both theoretical and experimental attention. They were extensively studied via spontaneous or induced fission reactions. Nuclei from this region of Segré chart exhibit vibrational, transitional, and rotational types of collectivity. The neutron-rich palladium and ruthenium nuclei, for example, show a typical transitional behavior while molybdenum isotopes exhibit a vibrational to near-rotational evolution [1, 2]. Such changes in the degree of collectivity are even stronger in the zirconium isotopic chain [1, 2] where the structure evolves from near-vibrational in ^{98}Zr to rotational-like in ^{104}Zr, the latter being the most deformed nucleus of the neutron-rich $Z = 40$ isotopes. As the next zirconium isotope ^{106}Zr is an $N = 66$ mid-shell nucleus, an even larger deformation can be expected.

A detailed analysis of some spectroscopic observables, such as the ratio $R_{4/2}$ of excitation energies of the first 2^+ and 4^+ levels [1, 2] or the amplitude of even-odd staggering in the γ band [2], shows that mid-shell effects in palladium isotopes occur in ^{114,116}Pd, *i.e.* two and four neutrons beyond $N = 66$. In the ruthenium isotopes these effects arise precisely at $N = 66$ while in the molybdenum chain they occur in ^{106}Mo, *i.e.* two neutrons before mid-shell. Furthermore, it was shown that the degree of collectivity decreases in the heavier $N = 66, 68$ molybdenum isotopes ^{108,110}Mo. In spite of the fact that the experimental information on the heavy zirconium nuclei is poor, it is clear that the degree of collectivity increases towards ^{104}Zr [1] which has 64 neutrons and is the heaviest zirconium isotope known to date. The shift of the mid-shell in the various isotopic chains was explained in Ref. [1] as resulting from the filling of the neutron $h_{11/2}$ and proton $g_{9/2}$ intruder orbitals.

Self-consistent calculations show that in the region of neutron-rich nuclei approaching the neutron-drip line, the single-particle shell structure may significantly change due to the diffuseness of the neutron density [3]. Also, as widely discussed in the literature, due to a predicted weakening of the spin-orbit force, new magic numbers may be expected in neutron-rich nuclei. For instance, in a study of $N = 82$ isotones, evidence for shell quenching was presented in Ref. [4]. On the other hand, Jungclaus *et al.* [5] argued that from the isomeric decay study in ^{130}Cd there is no direct evidence for the shell quenching in the region of the heavy cadmium nuclei.

The lower-Z $N = 82$ nuclei, however, have not yet been studied experimentally and the suppression of the shell effects in this region is still an open question. Properties of these nuclei were predicted within a relativistic Hartree-Fock Bogoliubov (HFB) approach [6]. The calculations, performed with different parametrizations, show that the $N = 82$ shell gap persists in the heavy palladium and ruthenium nuclei but that a weakening of this gap is expected in the zirconium isotopes. For example, the two-neutron separation energies from ^{118}Zr to ^{126}Zr, obtained via HFB calculations with the SkP interaction, show no discontinuity at $N = 82$ but a rather smooth behavior. As discussed above, nuclear collective behavior is expected to enhance towards the mid-shell as a result of the increase in valence particle number. If, however, the HFB+SkP scenario for the zirconium isotopes turns out to be valid and $N = 82$ vanishes or is weakened in the neutron-rich region, then the determination of valence-particle number is fraught with ambiguity, leading to a different behavior of nuclear collectivity in this isotopic chain. The aim of the present paper, therefore, is to predict the spectroscopic properties concerning the $N = 66$ mid-shell zirconium nucleus ^{106}Zr, based on the assumption that $N = 82$ remains a magic number in the heavy zirconium isotopes. Comparison with results of future experiments on this nucleus will then reveal whether this hypothesis is borne out or not.

II. MODEL

Often the only available information about neutron-rich nuclei comes from prompt γ-ray spectroscopy. The observed levels are grouped into $\Delta J = 2$ sequences, corresponding to the ground-state band, and/or into $\Delta J = 1$ sequences, based on a 2_2^+ level which usually is interpreted as a quasi-γ band [7]. Such structures naturally appear in the framework of the interacting boson model

(IBM) [8] which has been shown to be successful in the description of nuclear collective properties.

The IBM in its first version, known as IBM-1, is based on the assumption that nuclear collectivity can be expressed in terms of s and d bosons [8]. The model Hamiltonian is constructed from a set of 36 operators, bilinear in the boson creation and annihilation operators and generating the U(6) Lie algebra. Dynamical symmetries occur if the Hamiltonian can be written as a combination of invariant (or Casimir) operators of specific subalgebras of U(6) [9] and three such cases occur, namely the spherical vibrational limit U(5), the deformed limit SU(3), and γ-soft limit SO(6). These dynamical symmetries generate energy spectra with states that are labeled by the irreducible representations of the algebras in the respective chains that reduce the dynamical algebra U(6) into the symmetry algebra SO(3) of rotations in three-dimensional space. The different limits thus correspond to nuclei with distinct collective properties. For example, in the SO(6) limit the ground-state and γ bands lie in the same representation while in the SU(3) limit they are in different ones, leading to forbidden or weaker inter-band transitions in the latter case.

In the $A \approx 110$ nuclei of interest here strong transitions between the two bands are observed indicating that none of these nuclei can be interpreted in the exact SU(3) limit, but rather a transitional behavior should be expected. This can be achieved in the IBM-1 by the use of the full Hamiltonian which reads [8]

$$\hat{H} = \epsilon_d \hat{n}_d + \kappa\, \hat{Q}^\chi \cdot \hat{Q}^\chi + \kappa' \hat{L} \cdot \hat{L} + c_3 \hat{T}_3 \cdot \hat{T}_3 + c_4 \hat{T}_4 \cdot \hat{T}_4, \quad (1)$$

where $\hat{n}_d \equiv d^\dagger \cdot \tilde{d}$ and $\hat{L}_\mu \equiv \sqrt{10}[d^\dagger \times \tilde{d}]^{(1)}_\mu$ are the d-boson number and the angular momentum operators, respectively. Furthermore, the quadrupole operator is defined as $\hat{Q}^\chi_\mu \equiv [d^\dagger \times \tilde{s}]^{(2)}_\mu + \chi[d^\dagger \times \tilde{d}]^{(2)}_\mu$, while the last two terms in the Hamiltonian involve the operators $\hat{T}_{3,\mu} \equiv [d^\dagger \times \tilde{d}]^{(3)}_\mu$ and $\hat{T}_{4,\mu} \equiv [d^\dagger \times \tilde{d}]^{(4)}_\mu$. In the present work there is no need for the rotational term $\hat{L} \cdot \hat{L}$ and we take $\kappa' = 0$ throughout. The total number of bosons $N = n_s + n_d$ is taken as half the number of valence particles or holes, counted from the nearest closed-shell configuration, following the prescription of Ref. [10]. As such, IBM-1 calculations are indirectly related to the underlying shell structure. Finally, in the consistent-Q formalism [11] the operator for electric quadrupole transitions is introduced as $\hat{T}_\mu(\mathrm{E2}) = e_\mathrm{b} \hat{Q}^\chi_\mu$, where e_b is the boson effective charge and Q^χ_μ is the quadrupole operator with the same parameter χ as in the Hamiltonian (1).

III. RESULTS AND DISCUSSION

Since the addition or subtraction of a few nucleons may change significantly a nuclear spectrum, two nuclei with different numbers of valence neutrons and protons but with the same *total* number of valence nucleons—and hence the same number of bosons—may display different types of collectivity. In adjusting the parameters of the Hamiltonian (1) to spectra observed in a given region of the nuclear chart, it is therefore not sufficient to assume them to be constant for all nuclei since that would lead to identical spectra for nuclei with the same N. Instead, some dependence of the parameters on the *separate* neutron and proton boson numbers N_ν and N_π should be imposed. To avoid the complexity of determining the correct functional dependence on N_ν and N_π for each of the Hamiltonian parameters, we have followed the simpler procedure of separately considering chains of isotopes, isotones, or isobars that end with the nucleus of interest, ^{106}Zr, and fitting each chain with an independent set of parameters. This method avoids the problem of having identical spectra for constant boson number N (such nuclei belong to different chains) and, in addition, since the extrapolation to ^{106}Zr obtained from the different chains may vary, it gives an idea on the possible error of the prediction.

TABLE I: Parameters and rms deviation (in keV) for the $N = 66$ isotones and the $A = 106$ isobars.

	ϵ_d	κ	c_3	c_4	χ^a	rms
$N = 66$	1171	−24.3	−70.8	−134.9	−0.30	58
$A = 106$	1053	−25.6	−70.6	−118.3	−0.30	143

[a] Dimensionless.

In the present application to ^{106}Zr, the $N = 66$ isotonic chain includes γ-unstable ^{112}Pd, more triaxial ^{110}Ru, and near-rotational ^{108}Mo. The second set of nuclei belongs to the $A = 106$ isobaric chain [16] extending from vibrational-like ^{106}Pd to near-rotational ^{106}Mo. Unfortunately, the zirconium isotopic chain does not allow the determination of a unique set of model parameters since only yrast data are available for the neutron-rich isotopes ^{100,102,104}Zr. Consequently, only the isotonic and isobaric chains are considered in the fit. Nuclei in a given chain are distinguished by the number of bosons (*i.e.*, particle or hole pairs), counted from the nearest closed-shell configurations which are $Z = 28$ or $Z = 50$ for the protons, and $N = 50$ or $N = 82$ for the neutrons. Figure 1 summarizes known nuclei in the neighbourhood of ^{106}Zr. Nuclei with known excited levels are distinguished (full lines) from those of which only ground-state properties are known (dashed lines). Furthermore, the nuclei used in the fit are high-lighted with thick lines.

The model parameters ϵ_d, κ, c_3, and c_4, listed in Table I, are obtained after a least-squares fit to the experimental level energies. Since its effect on the excitation energies is weak, the parameter χ is varied independently to give a fair description of E2 transition rates in ^{106}Pd within the consistent-Q formalism, and other nuclei are calculated with the same value. Although within a given chain parameters may vary with boson number, any allowed variation does not markedly improve the quality of the fit. Consequently, to keep the number of parameters

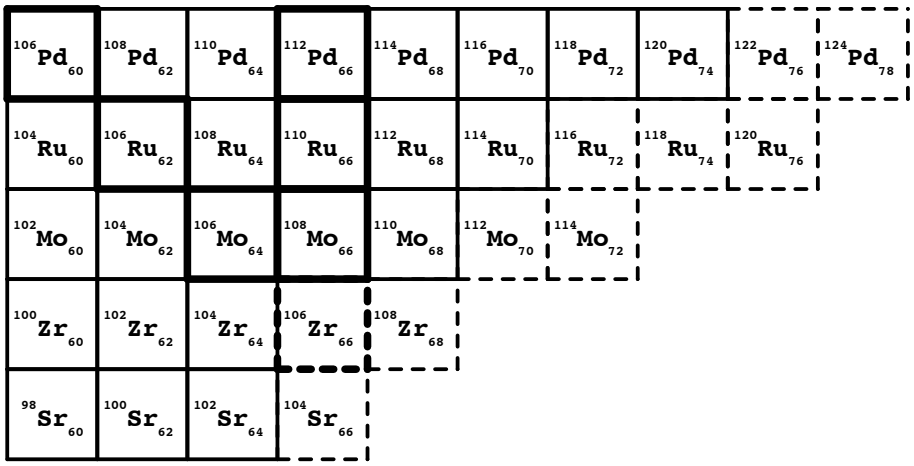

FIG. 1: Even-even nuclei in the region close to ^{106}Zr. All nuclei in boxes with full lines have known excited levels while those in boxes with broken lines are only known in their ground state. The nuclei used in the fit are in boxes with thick lines.

to a minimum, they are taken constant for a given chain and any structural evolution within that chain is due to the changing boson number N.

The quality of the fit is summarized by the root-mean-square (rms) deviation between the experimental and calculated level energies. The rms values obtained in the two independent fits are given in Table I. The experimental [12, 13, 14, 15, 16] and theoretical energies are listed in Tables II and III for the $N = 66$ and $A = 106$ chains, respectively. The nucleus ^{106}Pd is known in greater detail and is shown separately in Table IV. In both the isotopic and isobaric chains, the observed energy of the 2_1^+ state decreases when approaching the nucleus ^{106}Zr. The same trend is observed for the calculated energies as a function of boson number. The experimental energy of the γ-band head also decreases with increasing boson number and a similar evolution is observed for the 2_2^+ theoretical energies. According to the systematics of the less neutron-rich nuclei, the 2_1^+ level in ^{106}Zr should thus lie around 140 keV while the 2_2^+ level should be in the region 600–650 keV. Furthermore, the two different fits give approximately the same γ-band energies. Even though the two fitted parameter sets are close (see Table I), the $N = 66$ set gives rise to a slightly faster increase of the ground-state band energies than is the case for the $A = 106$ set.

The displacement of odd-spin with respect to even-spin γ-band levels can be quantified with the following function:

$$S(J) = E(J) - \frac{(J+1)E(J-1) + JE(J+1)}{2J+1}, \qquad (2)$$

where $E(J)$ is the energy of the level with angular momentum J. The experimental and theoretical staggering in the $N = 66$ isotones is plotted in Fig. 2; to gauge any systematic behavior, plots are drawn to the same scale. In general, the staggering amplitude is high for spherical nuclei and decreases towards the mid-shell region. The $N = 66$ isotones do not constitute an exception to the systematic trends established in Ref. [2]. The γ-unstable nucleus ^{112}Pd (10 bosons) shows the highest amplitude in $S(J)$ among the $N = 66$ isotones. The γ-band staggering is less pronounced in ^{110}Ru (11 bosons) while in ^{108}Mo (12 bosons) it is highly suppressed. From these systematics trends a γ band with a very low staggering amplitude is expected in ^{106}Zr, namely $S(J) \approx 10$ keV, which would make ^{106}Zr the nucleus with the lowest staggering amplitude observed in the $40 \leq Z \leq 50$ region.

Also electric quadrupole transition probabilities have been considered for the neutron-rich nuclei belonging to the $N = 66$ and $A = 106$ chains. The calculated values are listed in Tables V and VI along with the few known experimental values [16]. The boson effective charge $e_\mathrm{b} = 0.11$ eb is obtained after a least-squares fit to the B(E2) values measured in ^{106}Pd and this value is used for all other nuclei. The results show an increase of the $B(\mathrm{E2}; 2_1^+ \rightarrow 0_1^+)$ value from the near-vibrational ^{106}Pd towards the near-rotational ^{108}Mo. This B(E2) value is predicted highest for ^{106}Zr and the calculations for the two different chains give a consistent value of $B(E2; 2_1^+ \rightarrow 0_1^+) \approx 0.50$–$0.55$ e^{2}b^2. Furthermore, we note from Table VI the behavior predicted for the $B(E2; 2_2^+ \rightarrow 0_1^+)$ value which is small in ^{106}Pd and ^{106}Zr but becomes large for the isotopes in between, a characteristic feature of transitional nuclei.

IV. CONCLUSIONS

The aim of this paper was to illustrate the usefulness of the interacting boson model in its simplest version, the IBM-1, for predicting properties of exotic nuclei. The usual difficulty that arises with such attempts is that the variations of the model's parameters with the valence neutron and proton numbers are not known, pre-

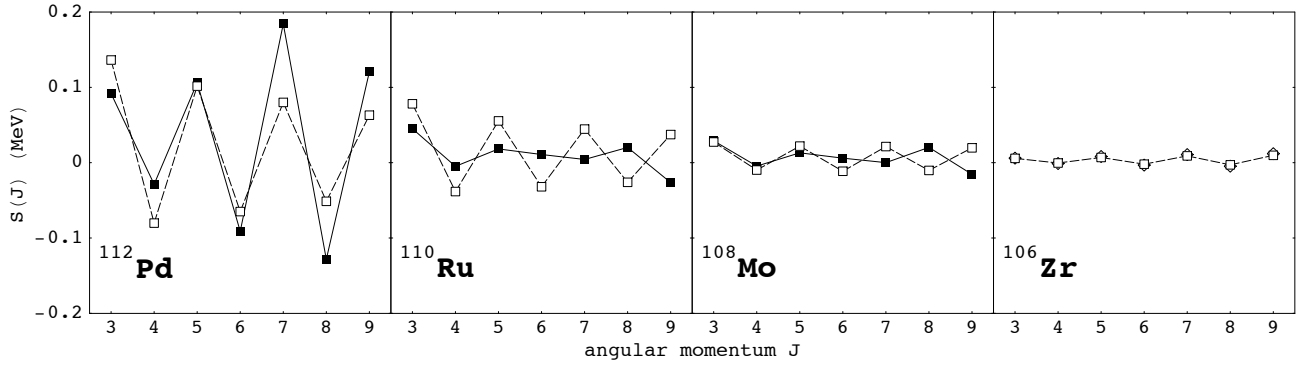

FIG. 2: Experimental (full symbols connected with full lines) and theoretical (open symbols connected with dashed lines) γ-band staggering $S(J)$ in the $N = 66$ isotones. In ^{106}Zr both near-identical predictions are shown based on the extrapolation of the $N = 66$ isotones (open squares) and of the $A = 106$ isobars (open diamonds).

TABLE II: Experimental and theoretical excitation energies (in keV) of levels in neutron-rich $N = 66$ isotones.

nucleus	$J^\pi_{\rm gsb}$	$E^{\rm ex}_{\rm gsb}$	$E^{\rm th}_{\rm gsb}$	J^π_γ	$E^{\rm ex}_\gamma$	$E^{\rm th}_\gamma$
^{112}Pd	0^+	0	0	2^+	736	775
($N = 10$)	2^+	348	354	3^+	1096	1138
	4^+	883	849	4^+	1362	1304
	6^+	1550	1481	5^+	1759	1692
	8^+	2318	2240	6^+	2002	1934
	10^+	3049	3118	7^+	2483	2357
				8^+	2638	2669
				9^+	3085	3129
				10^+	3327	3507
^{110}Ru	0^+	0	0	2^+	613	689
($N = 11$)	2^+	241	253	3^+	860	960
	4^+	663	671	4^+	1084	1139
	6^+	1239	1239	5^+	1375	1449
	8^+	1945	1945	6^+	1684	1699
	10^+	2759	2777	7^+	2021	2060
				8^+	2397	2377
				9^+	2777	2789
				10^+	3255	3168
^{108}Mo	0^+	0	0	2^+	586	647
($N = 12$)	2^+	193	178	3^+	783	830
	4^+	564	533	4^+	978	1010
	6^+	1090	1047	5^+	1232	1257
	8^+	1753	1705	6^+	1508	1505
	10^+	2529	2495	7^+	1817	1819
				8^+	2170	2132
				9^+	2524	2506
				10^+	2950	2880
^{106}Zr	0^+	0	0	2^+	—	618
($N = 13$)	2^+	—	141	3^+	—	754
	4^+	—	455	4^+	—	922
	6^+	—	926	5^+	—	1133
	8^+	—	1543	6^+	—	1371
	10^+	—	2297	7^+	—	1653
				8^+	—	1956
				9^+	—	2303
				10^+	—	2668

TABLE III: Experimental and theoretical excitation energies (in keV) of levels in neutron-rich $A = 106$ isobars.

nucleus	$J^\pi_{\rm gsb}$	$E^{\rm ex}_{\rm gsb}$	$E^{\rm th}_{\rm gsb}$	J^π_γ	$E^{\rm ex}_\gamma$	$E^{\rm th}_\gamma$
^{106}Ru	0^+	0	0	2^+	792	772
($N = 9$)	2^+	270	362	3^+	1092	1156
	4^+	715	865	4^+	1307	1308
	6^+	1296	1498	5^+	1641	1720
	8^+	1973	2252	6^+	1908	1943
	10^+	2705	3115	7^+	2284	2387
				8^+	2960	2676
^{106}Mo	0^+	0	0	2^+	711	651
($N = 11$)	2^+	172	205	3^+	885	881
	4^+	522	582	4^+	1068	1057
	6^+	1033	1110	5^+	1307	1338
	8^+	1688	1773	6^+	1563	1578
	10^+	2472	2559	7^+	1868	1916
				8^+	2194	2217
				9^+	2559	2608
				10^+	2951	2965
^{106}Zr	0^+	0	0	2^+	—	630
($N = 13$)	2^+	—	134	3^+	—	762
	4^+	—	433	4^+	—	924
	6^+	—	883	5^+	—	1129
	8^+	—	1473	6^+	—	1357
	10^+	—	2192	7^+	—	1630
				8^+	—	1919
				9^+	—	2254
				10^+	—	2601

cluding a reliable extrapolation to unknown regions of the nuclear chart. Our method proposes to circumvent this problem by studying the structural evolution in three different chains of nuclei, namely isotopic, isotonic, and isobaric ones, which cross at the nucleus of interest at the outskirts of the region of stable nuclei. Predictions are obtained by extrapolating the different chains to the exotic nucleus in question, and, in addition, a comparison of these extrapolations gives an idea of the errors involved.

TABLE IV: Experimental and theoretical excitation energies (in keV) of levels in ^{106}Pd.

nucleus	J^π	E_1	E_2	E_3	E_4	E_5
^{106}Pd	$0^+_{\rm ex}$	0	1134	1706	2001	2278
($N=7$)	$0^+_{\rm th}$	0	1017	1384	2080	2297
	$2^+_{\rm ex}$	512	1128	1562	1909	2242
	$2^+_{\rm th}$	519	982	1575	1859	2004
	$3^+_{\rm ex}$	1558				
	$3^+_{\rm th}$	1483				
	$4^+_{\rm ex}$	1229	1932	2077	2283	
	$4^+_{\rm th}$	1153	1617	2010	2213	
	$5^+_{\rm ex}$	2366				
	$5^+_{\rm th}$	2141				
	$6^+_{\rm ex}$	2077				
	$6^+_{\rm th}$	1896				

TABLE V: Theoretical B(E2) values (in units e^{2}b^2) for transitions in neutron-rich $N=66$ isotones.

transition	^{112}Pd	^{110}Ru	^{108}Mo	^{106}Zr
$2^+_1 \rightarrow 0^+_1$	0.27	0.35	0.45	0.53
$4^+_1 \rightarrow 2^+_1$	0.43	0.54	0.65	0.75
$0^+_2 \rightarrow 2^+_1$	0.22	0.17	0.057	0.003
$2^+_2 \rightarrow 0^+_1$	0.015	0.024	0.025	0.020

This method was applied to the neutron-rich members of the $N=66$ isotonic and $A=106$ isobaric chains of which level energies and electric quadrupole transition probabilities were fitted with IBM-1. The two chains intersect at ^{106}Zr which allowed the prediction of this nucleus' excitation energies and electric quadrupole transition properties.

As a final remark we emphasize that the IBM-1 is a valence-nucleon model and that the extrapolations as described here crucially depend on the definition of neighboring closed-shell configurations. Thus, the results on ^{106}Zr indirectly involve the assumption of the persistence of magic numbers in this region of neutron-rich nuclei.

V. ACKNOWLEDGMENTS

S.L. acknowledges the Bulgarian National Science Fund for a Research Fellowship Grant. This work was partially supported by the Agence National de Recherche, France, under contract nr ANR-07-BLAN-0256-03.

TABLE VI: Experimental and theoretical B(E2) values (in units e^{2}b^2) for transitions in neutron-rich $A=106$ isobars.

transition	^{106}Pd		^{106}Ru	^{106}Mo	^{106}Zr
	Expt	Theo	Theo	Theo	Theo
$2^+_1 \rightarrow 0^+_1$	0.134 (4)	0.14	0.23	0.37	0.54
$4^+_1 \rightarrow 2^+_1$	0.211 (17)	0.22	0.36	0.55	0.77
$0^+_2 \rightarrow 2^+_1$	0.105 (20)	0.13	0.16	0.092	0.0044
$2^+_2 \rightarrow 0^+_1$	0.0035 (3)	0.0019	0.0097	0.023	0.021

[1] W. Urban *et al.*, Eur. Phys. J. A **20**, 381 (2004).
[2] S. Lalkovski and N. Minkov, J. Phys. G: Nucl. Part. Phys. **31**, 427 (2005).
[3] J. Dobaczewski, I. Hamamoto, W. Nazarewicz, and J.A. Sheikh, Phys. Rev. Lett. **72**, 981 (1994).
[4] T. Kaurzsch *et al.*, Eur. Phys. J. A **9**, 201 (2000).
[5] A. Jungclaus *et al.*, Phys. Rev. Lett. **99**, 132501 (2007).
[6] M.M. Sharma and A.R. Farhan, Phys. Rev. C **65**, 044301 (2002).
[7] M. Sakai, At. Data Nucl. Data Tables **31**, 399 (1984).
[8] F. Iachello and A. Arima, *The Interacting Boson Model* (Cambridge University Press, Cambridge, 1987).
[9] F. Iachello, *Lie Algebras and Applications* (Springer-Verlag, Berlin, 2006).
[10] R.F. Casten, *Nuclear Structure from a Simple Perspective* (Oxford University Press, Oxford, 1990).
[11] D.D. Warner and R.F. Casten, Phys. Rev. Lett. **48**, 1385 (1982).
[12] R. Krücken *et al.*, Eur. Phys. J. A **10**, 151 (2001).
[13] D. DeFrenne and E. Jacobs, Nucl. Data Sheets **89**, 481 (2000).
[14] Jiang Zhuo *et al.*, Chin. Phys. Lett. **20**, 350 (2003).
[15] J. Blachot, Nucl. Data Sheets **91**, 135 (2000).
[16] D. DeFrenne and A. Negret, Nucl. Data Sheets **109**, 943 (2008).